was raised against glutathione S-transferase (GST) *Xenopus* Survivin and affinity purified using cleaved Survivin. Antibodies against hFAM were raised against each of four peptides (TPPDEQGQGDAPPQLED, CAPDEHESPPPEDAP, QRAQENYEGSEEVSPPQTKDQ, and GDEKQDNESNVDPRDDV) (*36*) and one GST fusion of the C-terminal fragment (amino acids 2347 to 2547) of hFAM. All were affinity purified against the respective antigens. Mouse Ufd1 was cloned into the pEF6/V5-His vector. Ufd1 antibodies were raised against GST-Ufd1 fusion protein and purified against His-tagged Ufd1. Antibodies against tubulin (Sigma), ACA (Antibodies Incorporated), human Survivin (R&D systems), human Aurora B (BD Biosciences), HA (Roche), Myc (Santa Cruz), and control immunoglobulin G (IgG) (Jackson Laboratory) were purchased. Antibodies against phosphorylated MCAK were described previously (*21*). Immunoprecipitation and immunofluorescence were carried out as described previously (*15*).

5. M. Jones *et al.*, *Hum. Mol. Genet.* **5**, 1695 (1996).
6. T. Noma *et al.*, *Mech. Dev.* **119S**, S91 (2002).
7. S. Wood *et al.*, *Mech. Dev.* **63**, 29 (1997).
8. J. Fischer-Vize, G. Rubin, R. Lehmann, *Development* **116**, 985 (1992).
9. Y. Huang, J. Fischer-Vize, *Development* **122**, 3207 (1996).
10. X. Chen, B. Zhang, J. Fischer, *Genes Dev.* **16**, 289 (2002).
11. A. Cadavid, A. Ginzel, J. Fischer, *Development* **127**, 1727 (2000).
12. Z. Wu, Q. Li, M. Fortini, J. Fischer, *Dev. Genet.* **25**, 312 (1999).
13. S. Taya *et al.*, *J. Cell Biol.* **142**, 1053 (1998).
14. R. Murray, L. Jolly, S. Wood, *Mol. Biol. Cell* **15**, 1591 (2003).
15. K. Cao, R. Nakajima, H. H. Meyer, Y. Zheng, *Cell* **115**, 355 (2003).
16. H. Richly *et al.*, *Cell* **120**, 73 (2005).
17. A. Carvalho, M. Carmena, C. Sambade, W. C. Earnshaw, S. P. Wheatley, *J. Cell Sci.* **116**, 2987 (2003).
18. RNA interference was carried out by transfecting HeLa, NIH 3T3, or human HEK 293 cells with 160 to 200 nM (final) siRNA (Dharmacon or Qiagen) corresponding to luciferase (CGTACGCGGAATACTTCGA), Survivin (GGACCACCGCATCTCTACA), hFAM (hFAM-s1: GCAGTGAGTGGCTGGAAG or hFAM-s2: ACTTCCTACCGAATGCAGA), or Ufd1 (Ufd1-S1: CTGGGCTACAAAGAACCCGAA or Ufd1-S2: CTGCGTGTGATGGAGACCAAA) (*36*) using Oligofectamine (Invitrogen). The cells were analyzed at 48 or 72 hours after transfection. For hFAM rescue experiments, HeLa cells were transfected with $pV5FAM^{INS}$, $pV5FAM^{WT}$, $pV5FAM^{CAT}$, or pV5 vector for at least 48 hours before siRNA transfection. Cells were analyzed 72 hours after siRNA transfection.
19. W. Earnshaw, B. Bordwell, C. Marino, N. Rothfield, *J. Clin. Invest.* **77**, 426 (1986).
20. R. Gassmann *et al.*, *J. Cell Biol.* **166**, 179 (2004).
21. P. Andrews *et al.*, *Dev. Cell* **6**, 253 (2004).
22. W. Lan *et al.*, *Curr. Biol.* **14**, 273 (2004).
23. H. Li, D. Wirtz, Y. Zheng, *J. Cell Biol.* **160**, 635 (2003).
24. HeLa cells were treated with hFAM-s1 or control siRNA for ~24 hours and then transfected with Survivin-GFP. FLIP or FRAP was carried out 48 to 72 hours after transfection. Detailed descriptions of the kinetic modeling of FLIP and FRAP can be found in (*26*).
25. M. Delacour-Larose, A. Mollar, D. A. Skoufias, R. L. Margolis, S. Dimitrov, *Cell Cycle* **3**, 1418 (2004).
26. Materials and methods are available as supporting materials on *Science* Online.
27. L. Sun, Z. Chen, *Curr. Opin. Cell Biol.* **16**, 119 (2004).
28. For ubiquitination assays, HeLa cells or HEK 293 cells were cotransfected with Myc-Survivin and HA-ubiquitin or the respective vector controls for 30 hours followed by nocodazole (400 nM final) arrest. Cell lysates were subjected to immunoprecipitation using antibody to Myc. Ubiquitinated Myc-Survivin was detected using antibody to HA. To assay the Dub activity of FAM, HeLa cells were cotransfected with Myc-Survivin, HA-ubiquitin, and $V5FAM^{CAT}$ or the respective vector controls followed by the same treatment and analyses described above.
29. X. J. Yang, *Oncogene* **3**, 653 (2005).
30. M. A. Verdecia *et al.*, *Nat. Struct. Biol.* **7**, 602 (2000).
31. C. Hoege, G.-L. Pfander, G. Pyrowolakis, S. Jentsch, *Nature* **419**, 135 (2002).
32. I. Wertz *et al.*, *Nature* **430**, 694 (2004).
33. J. Zhao, T. Tenev, L. Martins, J. Downward, N. Lemoine, *J. Cell Sci.* **23**, 4363 (2000).
34. C. Pickart, *Cell* **116**, 181 (2004).
35. S. Wing, *Inter. J. Biochem. Cell Biol.* **35**, 590 (2003).
36. Single-letter abbreviations for the amino acid residues are as follows: A, Ala; C, Cys; D, Asp; E, Glu; F, Phe; G, Gly; H, His; I, Ile; K, Lys; L, Leu; M, Met; N, Asn; P, Pro; Q, Gln; R, Arg; S, Ser; T, Thr; V, Val; W, Trp; and Y, Tyr.
37. We thank J. Swedlow, S. Wood, H. Meyer, and T. Dawson for antibodies and constructs; B. Lane for protein sequencing; C. Pickart for helpful advice on ubiquitination assays; O. Martin and R. Chen for excellent technical support; and M. Guo, D. Koshland, J. Yanowitz, and the members of Zheng lab for helpful comments. This work was supported by Howard Hughes Medical Institution and by National Institute of General Medical Sciences grant no. GM56312.

Supporting Online Material
www.sciencemag.org/cgi/content/full/310/5753/1499/DC1
Materials and Methods
Figs. S1 to S11
Tables S1 to S3
References

14 September 2005; accepted 25 October 2005
10.1126/science.1120160

Prostaglandin E_2 Promotes Colon Cancer Cell Growth Through a G_s-Axin-β-Catenin Signaling Axis

Maria Domenica Castellone,[1] Hidemi Teramoto,[2] Bart O. Williams,[3] Kirk M. Druey,[4] J. Silvio Gutkind[1]*

How cyclooxygenase-2 (COX-2) and its proinflammatory metabolite prostaglandin E2 (PGE2) enhance colon cancer progression remains poorly understood. We show that PGE2 stimulates colon cancer cell growth through its heterotrimeric guanine nucleotide-binding protein (G protein)–coupled receptor, EP2, by a signaling route that involves the activation of phosphoinositide 3-kinase and the protein kinase Akt by free G protein βγ subunits and the direct association of the G protein α_s subunit with the regulator of G protein signaling (RGS) domain of axin. This leads to the inactivation and release of glycogen synthase kinase 3β from its complex with axin, thereby relieving the inhibitory phosphorylation of β-catenin and activating its signaling pathway. These findings may provide a molecular framework for the future evaluation of chemopreventive strategies for colorectal cancer.

Colorectal cancer represents the third leading cause of cancer-related deaths in both men and women in the United States (*1*). The development of colon cancer results from the sequential accumulation of mutations or deletions in the coding sequence of a number of tumor-suppressor genes and oncogenes, together with aberrant activity of molecules controlling genomic stability (*2*). Patients with familial adenomatous polyposis, a disease characterized by the presence of numerous colorectal polyps, harbor germline mutations of one allele of the *adenomatous polyposis coli* (*APC*) tumor-suppressor gene and develop colon cancer upon mutational damage or loss of the wild-type allele (*3*). Like humans, mice with germline mutations in *APC*, Apc^{min} (multiple intestinal neoplasia) mice, are predisposed to the formation of intestinal adenomas (*4*). Loss of full-length APC proteins is also one of the earliest events occurring in sporadic colon cancer, suggesting that APC may act as a gatekeeper of the colonic epithelium. Nonsteroidal anti-inflammatory drugs (NSAIDs)—which inhibit two enzymes involved in prostaglandin biosynthesis, cyclooxygenase-1 (COX-1) and cyclooxygenase-2 (COX-2)—reduce the number and size of adenomas in patients with familial adenomatous polyposis and prevent colon cancer development in Apc^{min} mice (*5*). Indeed, emerging clinical and experimental evidence now supports a potent antitumorigenic efficacy of NSAIDs in colon cancer (*6*) and implicates the contribution of COX-2 and one of its metabolites, prostaglandin E2 (PGE2), in colon cancer development (*7*). How the

[1]Oral and Pharyngeal Cancer Branch, National Institute of Dental and Craniofacial Research, National Institutes of Health, Bethesda, MD 20892–4340, USA. [2]Kojin Hospital, 1-710 Shikenya, Moriyama, Nagoya 463-8530, Japan. [3]Laboratory of Cell Signaling and Carcinogenesis, Van Andel Research Institute, Grand Rapids, MI 49503, USA. [4]Molecular Signal Transduction Section, Laboratory of Allergic Diseases, National Institute of Allergy and Infectious Diseases, National Institutes of Health, Rockville, MD 20852, USA.

*To whom correspondence should be addressed. E-mail: sg39v@nih.gov

interplay between PGE2 and APC-regulated pathways leads to colon cancer cell growth remains poorly understood.

PGE2 is a potent mitogen in colon cancer cells (*8*), as reflected by its ability to stimulate the synthesis of DNA to an extent similar to that provoked by serum in DLD-1 cells, a colon cancer cell line homozygous for an inactivating mutation in *APC* (*9*) (fig. S1, A and B) (*10*). We and others (*11*) obtained similar results in a panel of colon cancer–derived cells. Although PGE2 can cause the indirect activation of EGF receptors (EGFR) (*12*), we observed only a minimal increase in the tyrosine phosphorylation of EGFRs upon PGE2 treatment. Furthermore, EGFR kinase inhibitors, such as AG1478, diminished the mitogenic response to EGF but did not prevent the stimulation of DNA synthesis in response to PGE2 or serum (supporting online text). These results indicate that PGE2 may also stimulate EGFR-independent cell growth pathway(s). Among them, we focused our attention on β-catenin, whose cytoplasmic stabilization contributes to colon cancer progression upon *APC* loss (*13*). Increased amounts of β-catenin protein lead to complex formation between β-catenin and members of the transcription factor family that includes the T cell factor (TCF) and lymphoid enhancer factor-1 (LEF) family of DNA-binding proteins, resulting in activation of target gene promoters (*13*).

PGE2 stimulated expression of a β-catenin/TCF/LEF-dependent reporter gene system, TOPflash (*14*, *15*), in colon cancer cells (Fig. 1B and fig. S1C). Similar results were recently reported by others while this study was under revision (*16*). Because PGE2 receptors are coupled to the G protein G_s, which causes accumulation of cyclic adenosine monophosphate (cAMP) and activates protein kinase A (PKA), we confirmed that PGE2 treatment or transfection of cells with the active catalytic subunit of PKA also stimulated the activity of a cAMP-responsive-element–driven reporter gene (CRE-luc) (Fig. 1A). However, PKA did not activate TOPflash (Fig. 1B). Similarly, accumulation of cAMP after activation of adenylyl cyclase with forskolin (*17*) promoted CRE-luc activation but not TOPflash reporter activity (Fig. 1, A and B). These results suggest that activation of PKA is not sufficient to stimulate the β-catenin pathway. Rather, activation of TOPflash by PGE2 correlated with the dephosphorylation of β-catenin and its accumulation and nuclear translocation (Fig. 1C). Furthermore, β-catenin was strictly required for the mitogenic activity of PGE2, because reduction of cellular concentration of β-catenin by a specific small interfering RNA (siRNA) inhibited the growth-promoting effect of this metabolic product of COX-2 (Fig. 1D).

Because EP2 receptors are central mediators of the responses to PGE2 in colon cancer cells (*7*, *18*), we tested whether these prostaglandin receptors promoted activation of β-catenin upon ectopic expression in human kidney embryonic epithelial HEK293T cells. We used β-adrenergic receptors, a prototypical G_s-coupled receptor (*19*), as a control. PGE2 and isoproterenol, a β-adrenergic agonist, stimulated both the CRE and TOPflash reporter systems (Fig. 2A). In contrast, forskolin, which increases intracellular cAMP, did not enhance TOPflash activity despite activating CRE-luc to a similar extent as did PGE2. Because EP2 and β-adrenergic receptors are coupled to G_s proteins, we tested whether the reporter activity could be increased by a constitutive active form of $G\alpha_s$ ($G\alpha_sQ227L$, $G\alpha_sQL$) (Fig. 2B). $G\alpha_sQL$ activated both CRE- and TOPflash-mediated luciferase activity in a dose-dependent manner. Activation of the β-catenin pathway required the constitutive activity of $G\alpha_s$, because expression of its wild-type form, $G\alpha_sWT$, or an active mutant of $G\alpha_{i2}$, $G\alpha_{i2}QL$, failed to stimulate TOPflash activity in HEK293T and colon cancer cells (fig. S2). However, specific inhibition of PKA by expression of PKI, a heat-stable inhibitor of PKA (*20*), abolished the activation of CRE by $G\alpha_sQL$

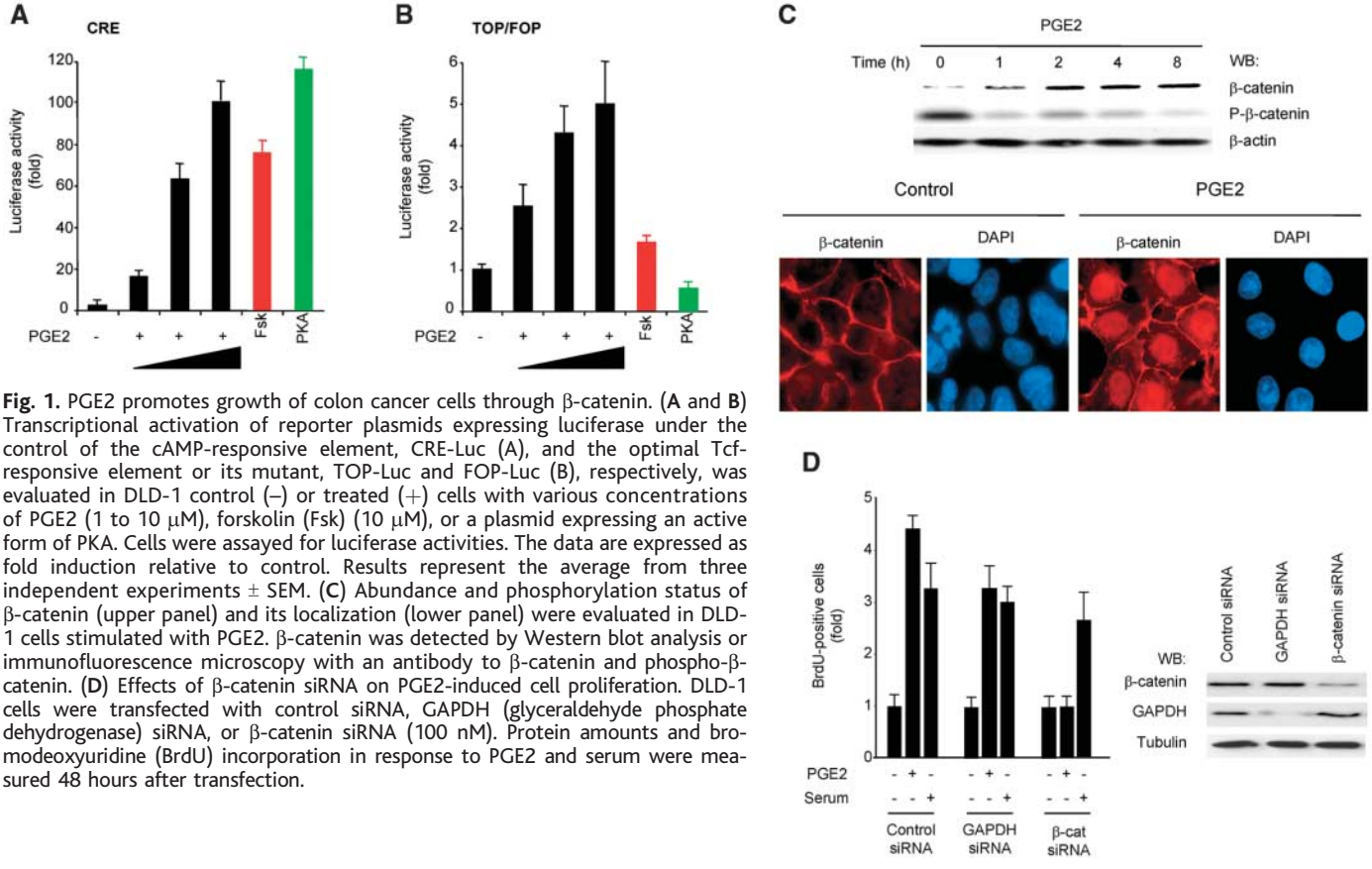

Fig. 1. PGE2 promotes growth of colon cancer cells through β-catenin. (**A** and **B**) Transcriptional activation of reporter plasmids expressing luciferase under the control of the cAMP-responsive element, CRE-Luc (A), and the optimal Tcf-responsive element or its mutant, TOP-Luc and FOP-Luc (B), respectively, was evaluated in DLD-1 control (–) or treated (+) cells with various concentrations of PGE2 (1 to 10 μM), forskolin (Fsk) (10 μM), or a plasmid expressing an active form of PKA. Cells were assayed for luciferase activities. The data are expressed as fold induction relative to control. Results represent the average from three independent experiments ± SEM. (**C**) Abundance and phosphorylation status of β-catenin (upper panel) and its localization (lower panel) were evaluated in DLD-1 cells stimulated with PGE2. β-catenin was detected by Western blot analysis or immunofluorescence microscopy with an antibody to β-catenin and phospho-β-catenin. (**D**) Effects of β-catenin siRNA on PGE2-induced cell proliferation. DLD-1 cells were transfected with control siRNA, GAPDH (glyceraldehyde phosphate dehydrogenase) siRNA, or β-catenin siRNA (100 nM). Protein amounts and bromodeoxyuridine (BrdU) incorporation in response to PGE2 and serum were measured 48 hours after transfection.

and PGE2 but not their activation of TOPflash (Fig. 2B). This result suggested that G_s-coupled receptors activate β-catenin through the $G\alpha_s$ protein but independently of cAMP and PKA.

The pathway leading to β-catenin activation by Wnt involves a complex series of events that results in the dissociation of β-catenin from axin, a scaffold protein that forms a large molecular complex with APC, the signal transducer disheveled (Dsh), and GSK-3β, a kinase that phosphorylates β-catenin, thereby promoting its ubiquitin-dependent proteolytic degradation (*21*). The importance of this inhibitory activity of axin is reinforced by the observation that inactivating mutations in axin are found in hepatocellular carcinomas (*22*). Axin binds APC through a regulator of G protein signaling (RGS) domain (*23*), which is similar in primary amino acid sequence and overall three-dimensional structure to other RGS proteins, whose best known function is to accelerate the guanosine triphosphatase (GTPase) activity of G proteins (*24*). However, the surface area of the axin RGS domain that binds APC is distinct from that used by other RGS proteins to bind G protein α subunits (*25*). This observation and the ability of G_s-coupled receptors to stimulate the transcriptional activity of β-catenin prompted us to explore whether the axin RGS domain may provide a direct link between $G\alpha_s$ and the β-catenin signaling axis. By overexpressing an epitope-tagged form of axin in HEK293T cells (fig. S3A), we observed that axin coimmunoprecipitated with $G\alpha_s$QL but not with the active form of $G\alpha_{i2}$ (Fig. 3, A and B). $G\alpha_s$ wild-type also coimmunoprecipitated with axin, but only when cells were treated with aluminum fluoride, which promotes Gα subunits to acquire a conformation that resembles their transition state, thus favoring RGS binding and GTPase activating protein (GAP) activity (*26*) (Fig. 3B). We next expressed epitope-tagged forms of individual axin domains, including the RGS domain, a region including the GSK-3β phosphorylation and binding sites, a β-catenin binding region, a protein phosphatase 2A (PP2A) binding area, and a DIX domain by which axin binds dsh (Fig. 3C and fig. S3B). Upon coexpression in HEK293T cells, only the RGS domain of axin was coimmunoprecipitated with $G\alpha_s$QL (Fig. 3C), indicating that axin interacts with $G\alpha_s$ through its RGS domain. Indeed, expression of a lentivirus encoding the axin RGS domain fused to green florescent protein (GFP) in DLD1 cells inhibited the activation of TOPflash evoked by PGE2 but not activation by an active mutant of β-catenin (Fig. 3D and fig. S3C). Expression of axin (RGS) also almost completely abolished the mitogenic activity of PGE2 but not the proliferative response to serum in these colon cancer cells (Fig. 3E).

To investigate whether the axin RGS domain binds $G\alpha_s$ directly, we expressed axin (RGS) as a glutathione *S*-transferase (GST)–fusion protein in bacteria and measured in vitro binding to recombinant six-histidine-tagged (H_6)-$G\alpha_s$. GST-RGS bound $G\alpha_s$ immobilized on nickel beads in an aluminum fluoride–dependent manner, as did an RGS protein that binds $G\alpha_s$ specifically, PX1 (RGS) (Fig. 3F, left panels). The guanosine diphosphate (GDP)–loaded, inactive form of $G\alpha_s$ also bound PX1 (RGS), albeit to a much lesser extent, as observed for other RGS proteins in vitro (*27*). By using GTPγS, a non-hydrolyzable GTP analog, we observed that $G\alpha_s$ does not bind to either RGS in its GTP-bound active state. A G_i-specific GAP, RGS19, did not bind $G\alpha_s$ under any condition. Nearly identical results were obtained in reciprocal experiments in which these bacterially expressed GST-RGS fusion proteins were precipitated with glutathione beads (Fig. 3F, left panels). As a control, recombinant $G\alpha_i$ efficiently bound GST-RGS19 in the presence of aluminum fluoride, but not to PX1 or axin (RGS) (Fig. 3F). These findings indicated that $G\alpha_s$ binds directly to the RGS domain of axin in a transition-state conformation.

Because axin bound $G\alpha_s$ in an aluminum fluoride–dependent manner, we evaluated whether axin could increase the GTPase activity of $G\alpha_s$. However, neither the RGS domain of axin nor full-length axin purified from baculovirus-infected Sf9 cells promoted the GTPase activity of $G\alpha_s$ during a single catalytic cycle of the enzyme (fig. S3D). Thus, additional accessory molecules or other modifications of axin could be required for its GAP activity, as is the case for other RGS proteins (*28*). It is also possible that the RGS domain of axin might be used primarily as a structural feature by which this scaffold protein can interact with and act as an effector for $G\alpha_s$, as do the RGS domain–containing RhoGEFs, which are effectors for G proteins of the $G\alpha_{12/13}$ family (*29*).

Because phosphorylation of β-catenin by GSK-3β leads to its rapid ubiquitination and subsequent degradation in the proteosome, inactivation of GSK-3β is often a prerequisite for stimulating the accumulation, nuclear translocation, and functional activity of β-catenin (*30*). Treatment of cells with PGE2 led to the rapid phosphorylation of GSK-3β on serine 9 (Fig. 4A and fig. S4), which inhibits its kinase activity (*31*). PGE2 also stimulated Akt activity in a PI3K-dependent manner (Fig. 4B). Because both PKA and Akt can phosphorylate GSK-3β at this inhibitory site (*32*), we tested whether PKA could mediate GSK-3β phosphorylation in response to PGE2. PKI did not prevent the phosphorylation of GSK-3β provoked by PGE2, but it diminished the GSK-3β phosphorylation induced by forskolin, indicating that PGE2 induces GSK-3β phos-

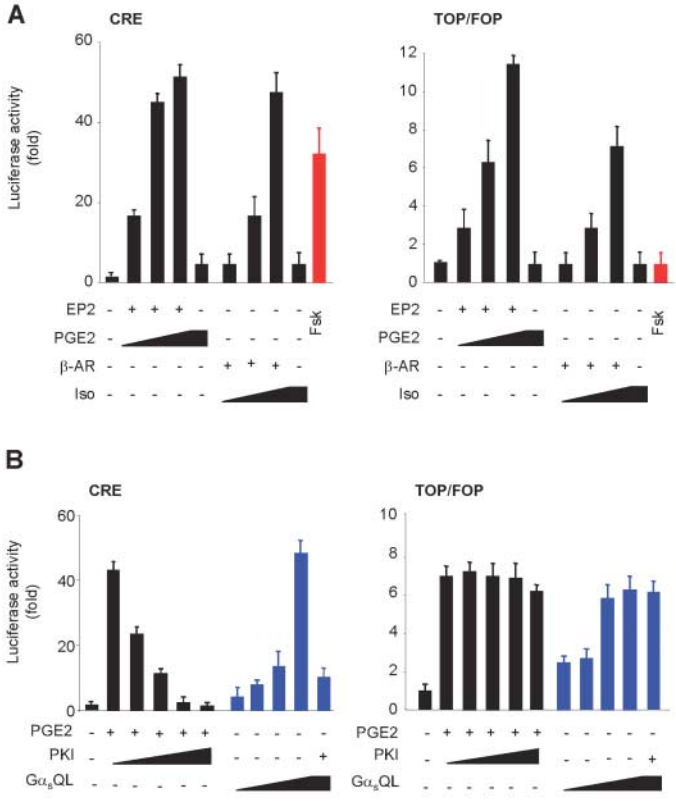

Fig. 2. G_s-coupled receptors (EP2 and β-adrenergic receptors) promote β-catenin activation independently of PKA. (**A**) Empty vector (–) or expression plasmids for EP2 or β-adrenergic receptor were transfected together with pGL3-CRE-Luc or pTOP and pFOP reporter plasmids. After 24 hours, cells were deprived of serum and stimulated with various concentrations of PGE2 (1 to 10 μM), isoproterenol (Iso) (10 to 100 μM), or forskolin (Fsk) (10 μM), as indicated, and assayed for dual luciferase activities. The data are expressed as fold increase relative to control ± SEM of a representative experiment that was repeated three times with nearly identical results. (**B**) TOP and FOP or CRE-Luc activities were also measured in EP2-expressing cells upon transfection of the vector alone or increasing concentrations (0.1 to 1 μg) of pCEFL-$G\alpha_s$QL or RSV-PKI in the absence (–) or presence (+) of PGE2 stimulation (1 μM).

phorylation independently of PKA (Fig. 4A). In contrast, blockade of the PI3K-Akt pathway by wortmannin (WM) abolished both basal and PGE2-induced phosphorylation of GSK-3β (Fig. 4B). Although PGE2 promotes nucleotide exchange on $G\alpha_s$ and subsequent dissociation of GTP-bound $G\alpha_s$ from Gβγ subunits, GTP-bound $G\alpha_s$ does not activate PI3K and Akt (*33*). Thus, we tested whether expression of the C-terminal domain of βark (βARK-C), which causes sequestration of Gβγ subunits (*34*), could inhibit phosphorylation of GSK-3β and Akt. Overexpression of βARK-C did not affect basal phosphorylation of Akt or GSK-3β but abolished the accumulation of their phosphorylated species upon PGE2 stimulation (Fig. 4B). βARK-C did not affect the phosphorylation of Akt and GSK-3β evoked by insulin, and neither WM nor βARK-C affected the activation of the CRE reporter by PGE2 (Fig. 4C), which is dependent on $G\alpha_s$ and cAMP.

Inhibition of GSK-3β phosphorylation by WM or βARK-C only partially reduced the activation of the β-catenin pathway by PGE2 (Fig. 4C), even when both treatments were combined. The view that GSK-3β phosphorylation is required for β-catenin activation has been challenged by experiments using knock-in mice homozygous for both a mutant GSK-3β lacking serine 9 and a mutant for the related GSK-3α lacking serine 21. These mice displayed normal regulation of the Wnt-β-catenin pathway (*35*). Likewise, GSK-3β phosphorylation may not be alone sufficient to stimulate β-catenin, as suggested by the findings that insulin promotes the phosphorylation of GSK-3β but not β-catenin activation (*36*) and that forskolin causes the PKA-dependent phosphorylation of GSK-3β but does not stimulate the TOPflash reporter effectively. Our data suggest that β-catenin stabilization by PGE2 occurs at least through two coordinated mechanisms, one initiated by Gβγ through PI3K, Akt, and the consequent phosphorylation and inactivation of GSK-3β, and another pathway initiated by $G\alpha_s$ that is independent of both GSK-3β phosphorylation and PKA activation.

GSK-3β appears to phosphorylate β-catenin primarily when it is bound to axin (*37*). We observed that GSK-3β coimmunoprecipitated with endogenous axin in both HEK293T and colon cancer cells (Fig. 4, D and E). However, stimulation of cells with PGE2 or expression of activated forms of $G\alpha_s$ was associated with reduced amounts of GSK-3β bound to

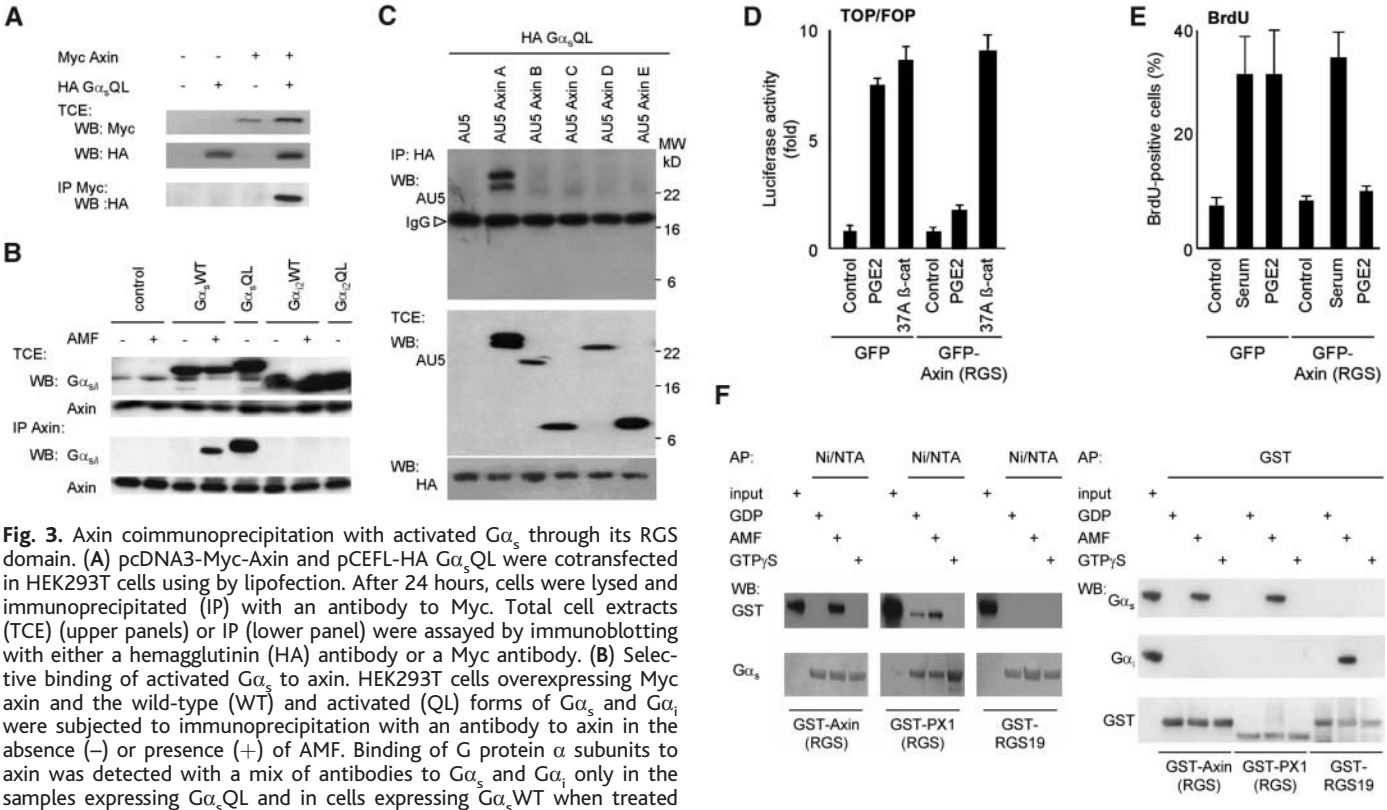

Fig. 3. Axin coimmunoprecipitation with activated $G\alpha_s$ through its RGS domain. (**A**) pcDNA3-Myc-Axin and pCEFL-HA $G\alpha_s$QL were cotransfected in HEK293T cells using by lipofection. After 24 hours, cells were lysed and immunoprecipitated (IP) with an antibody to Myc. Total cell extracts (TCE) (upper panels) or IP (lower panel) were assayed by immunoblotting with either a hemagglutinin (HA) antibody or a Myc antibody. (**B**) Selective binding of activated $G\alpha_s$ to axin. HEK293T cells overexpressing Myc axin and the wild-type (WT) and activated (QL) forms of $G\alpha_s$ and $G\alpha_i$ were subjected to immunoprecipitation with an antibody to axin in the absence (–) or presence (+) of AMF. Binding of G protein α subunits to axin was detected with a mix of antibodies to $G\alpha_s$ and $G\alpha_i$ only in the samples expressing $G\alpha_s$QL and in cells expressing $G\alpha_s$WT when treated with AMF. HA $G\alpha_s$QL was used for these experiments, hence its slightly higher molecular weight. (**C**) Immunoprecipitation of axin RGS domain with $G\alpha_s$QL. Vector-alone (AU5), or epitope-tagged forms of individual axin domains, including the RGS domain (A), a region including the GSK-3β phosphorylation and binding sites (B), a β-catenin binding region (C), a PP2A binding area (D), and a DIX domain by which axin binds dsh (E), were cotransfected with pCEFL-HA $G\alpha_s$QL. After 24 hours, cells were lysed and immunoprecipitated with an antibody to HA and analyzed by Western blotting with antibody to AU5 (upper panel). Total cell extracts were immunoblotted with either AU5 or HA antibody (lower panels). A band corresponding to the anti-HA immunoglobulin G (IgG) is depicted by an empty arrowhead. The position of the molecular size markers is indicated. (**D** and **E**) Axin-RGS domain inhibits the activation of the β-catenin pathway by PGE2, as well as its mitogenic effect. (D) Luciferase activity was measured in GFP and GFP-Axin RGS–infected DLD-1 cells transfected with the TOP and FOP reporter plasmids and stimulated with PGE2 (1 μM). Luciferase expression in cell lysates is represented as in Fig. 1. Transfection of an activated mutant of β-catenin (37A β-cat) was used as a control. (E) DNA synthesis was also measured as described in Fig. 1. The data were averaged from three independent experiments ± SEM, in which at least 500 cells were counted. (**F**) In vitro binding of axin to activated $G\alpha_s$ but not $G\alpha_i$. Left: Recombinant $His_6G\alpha_s$ was immobilized on Ni^{++} agarose (Ni/NTA) in the presence of GDP, aluminum magnesium fluoride (AMF), or GTPγS, and incubated with recombinant GST-Axin (RGS domain), GST-PX1 (RGS), or GST-RGS19 (GAIP). After bead washing, bound proteins were identified by immunoblotting with antibody to $G\alpha_s$ (top) or antibody to GST (bottom), running half of the total purified GST-fusion protein used for the experiment (input) as a control. Right: The indicated bacterially expressed GST-fusion proteins were purified and incubated in vitro with $His_6G\alpha_s$ or $G\alpha_{i1}$ and affinity-precipitated with glutathione agarose. Recombinant proteins bound to beads after extensive washing were detected with the indicated antibodies. Half of the total purified $His_6G\alpha_s$ or $G\alpha_{i1}$ used for the experiment (input) was run as a control. Figures represent four similar experiments.

axin without affecting the total amount of GSK-3β (Fig. 4, D and E). Because the GSK-binding site on axin is close to the RGS domain, we tested whether $G\alpha_s$ interaction with axin competes for GSK-3β binding in experiments with recombinant proteins. However, a 10-fold molar excess $G\alpha_s$-AMF (aluminum magnesium fluoride) did not reduce association of axin-H_6 with recombinant GSK-3β, suggesting that additional factors may be required for the dissociation of axin-GSK-3β complexes.

To test whether displacing GSK-3β from axin is sufficient to stimulate the β-catenin pathway, we first reduced the cellular concentration of GSK-3β and axin by specific siRNAs. Knockdown of axin or GSK-3β activated the TOPflash reporter (Fig. 5A and fig. S5A). Furthermore, the GSK-3 binding region of axin, but not the axin RGS as a control, bound GSK-3β and displaced it from its binding to axin (Fig. 5B and fig. S5B). This resulted in an increase in β-catenin activity similar to that stimulated by PGE2. Thus, the ability of PGE2 and $G\alpha_s$ to promote the release of GSK-3β from axin-containing complexes may represent an alternative mechanism to inhibit the functional activity of GSK-3β independently of phosphorylation.

These observations may have important implications for the study of β-catenin activation by Wnt, which involves two cell surface receptors, an LDL-containing single-pass transmembrane protein, LRP5 or LRP6, and a seven-transmembrane receptor, Frizzled (*38*, *39*). Whereas LRP5 and LRP6 appear to bind axin directly, how Frizzled signals to the canonical β-catenin pathway is still unclear. Frizzled may activate heterotrimeric G proteins (*40*), thus raising the possibility that the association of G protein α subunits with the RGS domain of axin may represent a point of convergence between the Wnt and prostaglandin-initiated pathways leading to β-catenin activation. On the other hand, how this process can be regulated by APC is at the present unknown. In our in vitro experiments, a peptide containing the primary sequence of APC that binds to axin RGS (*23*) did not compete for $G\alpha_s$ binding to axin (RGS). This is consistent with a distinct binding surface area for APC and $G\alpha_s$ on the axin RGS domain as predicted by the crystal structure (*25*). In contrast, expression of APC in colon cancer cells inhibited the activation of the β-catenin reporter system by PGE2. Considering that the tumor-promoting effect of PGE2 becomes evident only in the absence of functional APC, it is conceivable that APC may act by limiting the activation of β-catenin by prostaglandins, which are normally released in the colon in response to bacterial infection and proinflammatory substances. APC may bind the axin RGS domain and hinder the access of Gα subunits to this RGS. Alternatively, as APC interacts with β-catenin through numerous binding motifs, it may sequester free β-catenin, once it has been released from axin, and promote its turnover (*41*), thus raising the threshold of EP2 activation that is required to stimulate β-catenin–dependent gene expression.

Our studies indicate that in the absence of a functional APC, PGE2 can stimulate the proliferation of colon cancer cells by activating the β-catenin axis through a biochemical pathway initiated by the activation of the G protein–linked PGE2 receptor, EP2 (Fig. 6). PGE2 stimulation leads to the association of the activated α subunit of G_s with the RGS domain of axin, promoting release of GSK-3β from its complex with axin. Concurrently, free Gβγ subunits liberated upon $G\alpha_s$ activation

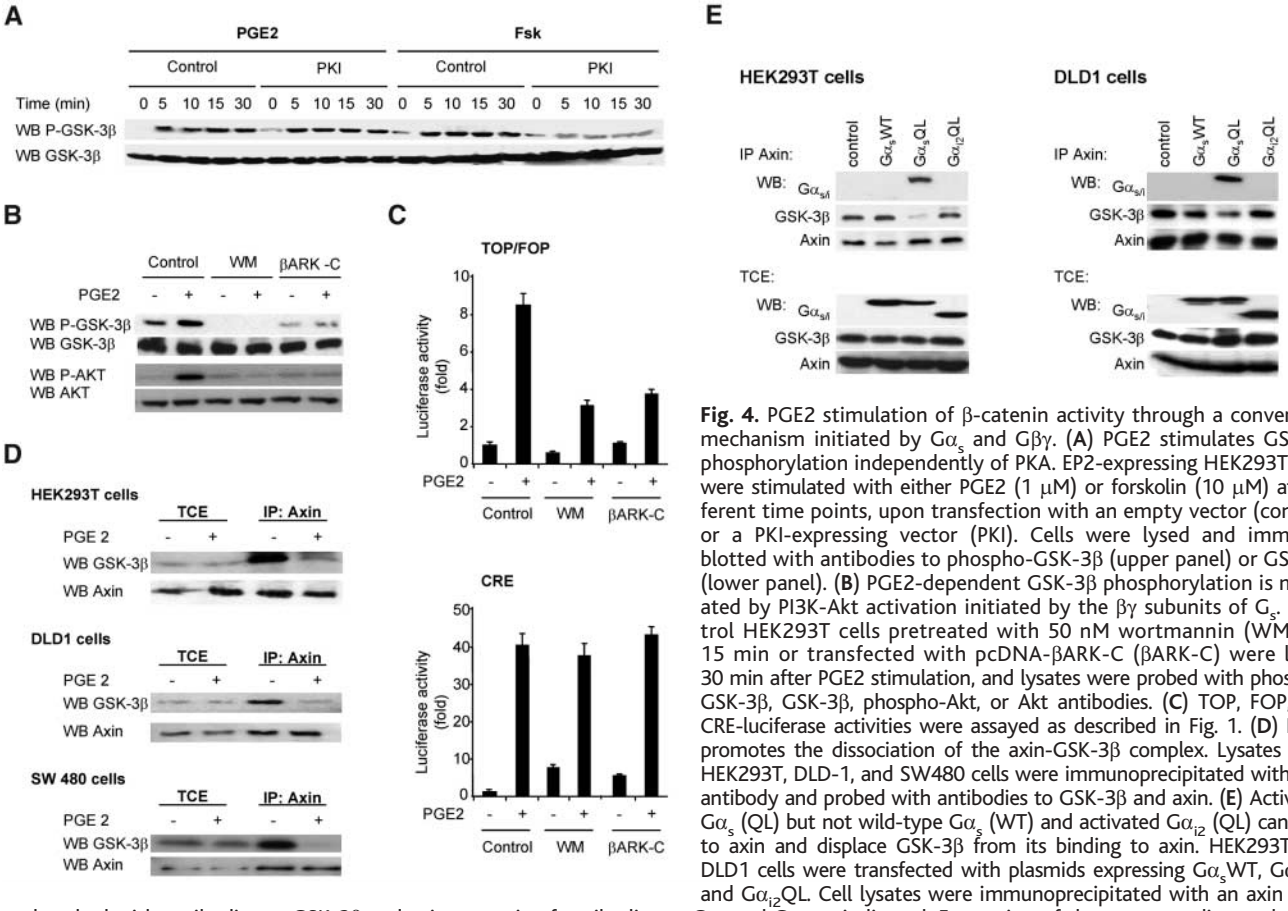

Fig. 4. PGE2 stimulation of β-catenin activity through a convergent mechanism initiated by $G\alpha_s$ and Gβγ. (**A**) PGE2 stimulates GSK-3β phosphorylation independently of PKA. EP2-expressing HEK293T cells were stimulated with either PGE2 (1 μM) or forskolin (10 μM) at different time points, upon transfection with an empty vector (control) or a PKI-expressing vector (PKI). Cells were lysed and immunoblotted with antibodies to phospho-GSK-3β (upper panel) or GSK-3β (lower panel). (**B**) PGE2-dependent GSK-3β phosphorylation is mediated by PI3K-Akt activation initiated by the βγ subunits of G_s. Control HEK293T cells pretreated with 50 nM wortmannin (WM) for 15 min or transfected with pcDNA-βARK-C (βARK-C) were lysed 30 min after PGE2 stimulation, and lysates were probed with phospho-GSK-3β, GSK-3β, phospho-Akt, or Akt antibodies. (**C**) TOP, FOP, and CRE-luciferase activities were assayed as described in Fig. 1. (**D**) PGE2 promotes the dissociation of the axin-GSK-3β complex. Lysates from HEK293T, DLD-1, and SW480 cells were immunoprecipitated with axin antibody and probed with antibodies to GSK-3β and axin. (**E**) Activated $G\alpha_s$ (QL) but not wild-type $G\alpha_s$ (WT) and activated $G\alpha_{i2}$ (QL) can bind to axin and displace GSK-3β from its binding to axin. HEK293T and DLD1 cells were transfected with plasmids expressing $G\alpha_s$WT, $G\alpha_s$QL, and $G\alpha_{i2}$QL. Cell lysates were immunoprecipitated with an axin antibody and probed with antibodies to GSK-3β and axin or a mix of antibodies to $G\alpha_s$ and $G\alpha_i$, as indicated. Expression of the corresponding molecules was also evaluated in total cell extracts (TCE).

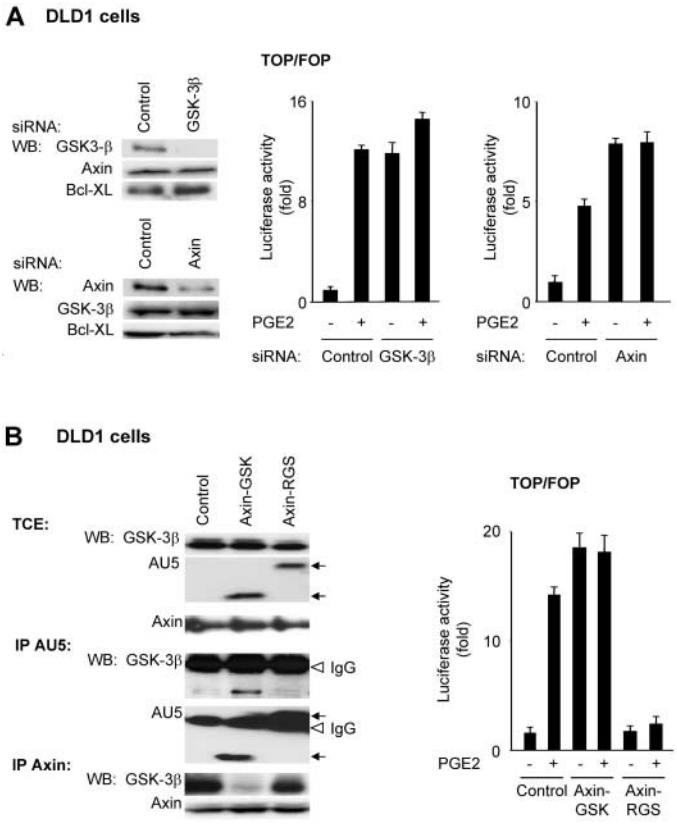

Fig. 5. Knockdown of axin or GSK-3β, or displacement of GSK-3β from axin, is sufficient to stimulate the β-catenin pathway in DLD1 colon cancer cells. (**A**) Knockdown of GSK-3β or axin in DLD1 cells stimulates β-catenin to a similar extent as PGE2 stimulation. Cells were transfected with the indicated siRNAs, and the expression of endogenous axin or GSK-3β was evaluated by Western blot analysis (left panels). Western blot analysis of Bcl-xL was used as a control. Luciferase expression was measured in cells transfected with the TOP and FOP reporter plasmids and the indicated siRNAs, with (+) or without (–) stimulation with PGE2 (1 μM), as in Fig. 1C (right panels). (**B**) Expression of the isolated GSK-3β binding region of axin is sufficient to displace GSK-3β from axin and stimulate β-catenin signaling. The GSK-3β binding region of axin [depicted as (B) in fig. S3] binds GSK-3β in vivo and displaces it from its binding to endogenous axin (left panel). The axin RGS domain [depicted as (A) in fig. S3)], which does not bind GSK-3β, served as a control. Arrows point to the epitope-tagged forms of the indicated axin regions. A band corresponding to the anti-HA IgG is depicted by an empty arrowhead. Cells were transfected with the TOP and FOP reporter plasmids together with the vector control or the expression vectors for the isolated axin domains and either left untreated (–) or stimulated with PGE2 (1 μM) (+). Luciferase expression was measured and represented as in Fig. 1B (right panel).

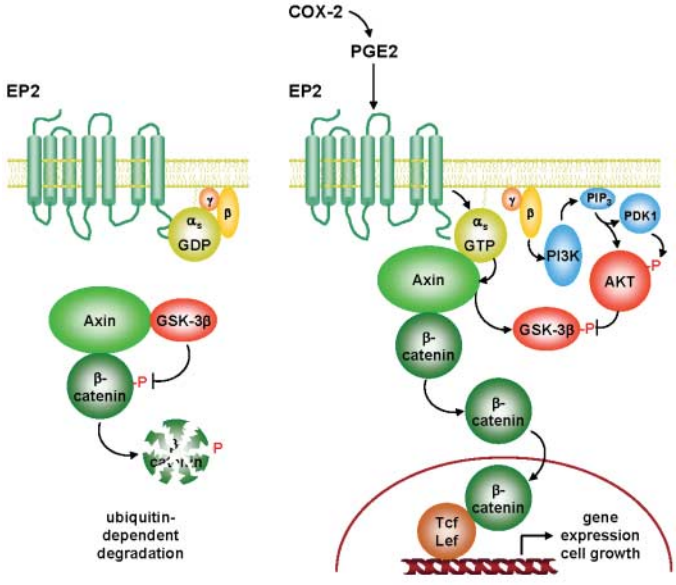

Fig. 6. Schematic representation of β-catenin pathway activation in response to PGE2. In the basal state (left panel), a cytoplasmic protein complex containing GSK-3β and axin promotes the inhibitory phosphorylation and consequent ubiquitin-dependent degradation of β-catenin in the proteasome. Overexpression of COX-2 in colon cancer cells and during inflammatory processes leads to the production of PGE2, which can activate EP2 receptors that are coupled to heterotrimeric G proteins of the G_s family (right panel). Upon exchange of GDP for GTP, the α subunit of G_s binds the RGS domain of axin, thereby promoting the release of GSK-3β from the complex. Concomitantly, free βγ subunits stimulate the PI3K-PDK1-Akt signaling route, which causes the phosphorylation and inactivation of GSK-3β. These events lead to the stabilization and nuclear translocation of β-catenin and to the expression of growth-promoting genes regulated by the Tcf and LEF family of transcription factors.

directly stimulate the activity of PI3K and Akt, leading to phosphorylation and inactivation of GSK-3β. Ultimately, these processes result in the stabilization and nuclear translocation of β-catenin, thereby stimulating LEF and β-catenin–dependent gene expression and the aberrant growth of colon cancer cells. These findings support the existence of a direct molecular mechanism by which COX-2 and inflammation can promote the progression of colon cancer, thus providing a molecular framework for the future clinical evaluation of NSAIDs as chemopreventive strategies for this devastating disease.

References and Notes

1. A. Jemal *et al.*, *CA Cancer J. Clin.* **55**, 10 (2005).
2. B. Vogelstein, K. W. Kinzler, *Nat. Med.* **10**, 789 (2004).
3. D. B. Levy *et al.*, *Cancer Res.* **54**, 5953 (1994).
4. M. Oshima *et al.*, *Proc. Natl. Acad. Sci. U.S.A.* **92**, 4482 (1995).
5. C. J. Torrance *et al.*, *Nat. Med.* **6**, 1024 (2000).
6. J. R. Brown, R. N. DuBois, *J. Clin. Oncol.* **23**, 2840 (2005).
7. M. Sonoshita *et al.*, *Nat. Med.* **7**, 1048 (2001).
8. D. Wang, F. G. Buchanan, H. Wang, S. K. Dey, R. N. DuBois, *Cancer Res.* **65**, 1822 (2005).
9. F. Cong, J. Zhang, W. Pao, P. Zhou, H. Varmus, *BMC Mol. Biol.* **4**, 10 (2003).
10. Materials and methods are available as supporting material on *Science* Online.
11. L. Qiao *et al.*, *Biochim. Biophys. Acta* **1258**, 215 (1995).
12. R. Pai *et al.*, *Nat. Med.* **8**, 289 (2002).
13. O. Tetsu, F. McCormick, *Nature* **398**, 422 (1999).
14. V. Korinek *et al.*, *Science* **275**, 1784 (1997).
15. H. Fujino, K. A. West, J. W. Regan, *J. Biol. Chem.* **277**, 2614 (2002).
16. J. Shao, C. Jung, C. Liu, H. Sheng, *J. Biol. Chem.* **280**, 26565 (2005).
17. K. B. Seamon, J. W. Daly, *Adv. Cyclic Nucleotide Protein Phosphorylation Res.* **20**, 1 (1986).
18. M. B. Hansen-Petrik *et al.*, *Cancer Res.* **62**, 403 (2002).
19. K. L. Pierce, R. T. Premont, R. J. Lefkowitz, *Nat. Rev. Mol. Cell Biol.* **3**, 639 (2002).
20. R. N. Day, J. A. Walder, R. A. Maurer, *J. Biol. Chem.* **264**, 431 (1989).
21. M. J. Hart, R. de los Santos, I. N. Albert, B. Rubinfeld, P. Polakis, *Curr. Biol.* **8**, 573 (1998).
22. S. Satoh *et al.*, *Nat. Genet.* **24**, 245 (2000).
23. K. E. Spink, P. Polakis, W. I. Weis, *EMBO J.* **19**, 2270 (2000).
24. D. M. Berman, A. G. Gilman, *J. Biol. Chem.* **273**, 1269 (1998).
25. R. Sterne-Marr *et al.*, *J. Biol. Chem.* **278**, 6050 (2003).
26. J. J. Tesmer, D. M. Berman, A. G. Gilman, S. R. Sprang, *Cell* **89**, 251 (1997).
27. N. Watson, M. E. Linder, K. M. Druey, J. H. Kehrl, K. J. Blumer, *Nature* **383**, 172 (1996).
28. T. Ingi *et al.*, *J. Neurosci.* **18**, 7178 (1998).
29. S. Tanabe, B. Kreutz, N. Suzuki, T. Kozasa, *Methods Enzymol.* **390**, 285 (2004).
30. B. Rubinfeld *et al.*, *Science* **272**, 1023 (1996).
31. V. Stambolic, J. R. Woodgett, *Biochem. J.* **303**, 701 (1994).
32. X. Fang *et al.*, *Proc. Natl. Acad. Sci. U.S.A.* **97**, 11960 (2000).
33. C. Murga, L. Laguinge, R. Wetzker, A. Cuadrado, J. S. Gutkind, *J. Biol. Chem.* **273**, 19080 (1998).
34. P. Crespo, T. G. Cachero, N. Xu, J. S. Gutkind, *J. Biol. Chem.* **270**, 25259 (1995).
35. E. J. McManus *et al.*, *EMBO J.* **24**, 1571 (2005).
36. V. W. Ding, R. H. Chen, F. McCormick, *J. Biol. Chem.* **275**, 32475 (2000).
37. S. Ikeda *et al.*, *EMBO J.* **17**, 1371 (1998).

38. X. He, M. Semenov, K. Tamai, X. Zeng, *Development* **131**, 1663 (2004).
39. G. Liu, A. Bafico, V. K. Harris, S. A. Aaronson, *Mol. Cell. Biol.* **23**, 5825 (2003).
40. T. Liu *et al.*, *Science* **292**, 1718 (2001).
41. Y. Xing, W. K. Clements, D. Kimelman, W. Xu, *Genes Dev.* **17**, 2753 (2003).
42. This research was partially supported by the Intramural Research Program of NIH, National Institute of Dental and Craniofacial Research.

Supporting Online Material
www.sciencemag.org/cgi/content/full/310/5753/1504/DC1
Materials and Methods
SOM Text
Figs. S1 to S5
References

16 June 2005; accepted 2 November 2005
Published online 17 November 2005
10.1126/science.1116221
Include this information when citing this paper.

Divergent Immunoglobulin G Subclass Activity Through Selective Fc Receptor Binding

Falk Nimmerjahn and Jeffrey V. Ravetch*

Subclasses of immunoglobulin G (IgG) display substantial differences in their ability to mediate effector responses, contributing to variable activity of antibodies against microbes and tumors. We demonstrate that the mechanism underlying this long-standing observation of subclass dominance in function is provided by the differential affinities of IgG subclasses for specific activating IgG Fc receptors compared with their affinities for the inhibitory IgG Fc receptor. The significant differences in the ratios of activating-to-inhibitory receptor binding predicted the in vivo activity. We suggest that these highly predictable functions assigned by Fc binding will be an important consideration in the design of therapeutic antibodies and vaccines.

Antibodies have evolved into classes with specific assigned functions. Within these classes, further subclassification extends immunoglobulin diversity, most strikingly in the four subclasses of IgG of mammals (*1*). In rodents and primates, these subclasses have evolved specialized effector responses, such as cytotoxicity, phagocytosis, and release of inflammatory mediators (*2*, *3*). IgG subclass expression is influenced by multiple factors, including the prevailing cytokine environment. For example, the T helper cell T_H2 cytokine interleukin 4 (IL-4) preferentially induces switching to IgG1 and IgE, whereas transforming growth factor–β (TGF-β) induces switching to IgG2b and IgA (*4*–*6*). Alternatively, T_H1 cytokines such as interferon-γ (IFN-γ) result in IgG2a, 2b, and 3 switching (*7*). Switching is also strongly influenced by the nature of the stimulating antigen. For example, protein antigens elicit a thymus-dependent response generally dominated by IgG1, 2a, and 2b, whereas carbohydrate antigens can induce so-called thymus-independent responses that result in IgG3 antibody expression (*8*). Among IgG subclasses, IgG2a and 2b are generally considered to be the most potent for activating effector responses and dominate antiviral immunity and autoimmune diseases (*9*–*11*). Such functional distinctions among these IgG subclasses have been attributed to differences in their capacity to fix complement (*12*, *13*). However, studies in complement-deficient mice have challenged this assumption and have focused attention on the cellular receptors for IgG, the FcγRs, as the primary mediators of IgG effector responses (*14*, *15*). We hypothesized that unified mechanisms accounting for the different potencies of IgG subclasses might be based on the differential binding to the known FcRs.

Activation FcγRs are expressed on all myeloid cells, and their cross-linking results in sustained cellular responses (*3*). Balancing these activation receptors is the inhibitory Fc receptor, FcγRIIB, which, when coligated to activation receptors, dampens the cellular response (*3*, *16*). The coexpression of activation and inhibitory receptors establishes a threshold for cellular triggering by IgG antibodies. Although all FcγRs can bind IgG immune complexes, we have observed that individual Fc receptors display significantly different affinities for IgG subclasses (*17*). We described this differential affinity for functionally distinct FcRs by specific IgG subclasses as a ratio, referred to as the activating-to-inhibitory (or A/I) ratio (*17*). These A/I ratios were found to differ by several orders of magnitude between IgG subclasses and thus raised the possibility that the variation in in vivo IgG subclass activity could be directly linked to the specific A/I ratio. To address this hypothesis, we established an in vivo system for testing antibodies that differed in their A/I ratios. The variable portions of the immunoglobulin heavy chain (V_H regions) of the cloned hybridomas that recognize either the melanosome gp75 antigen (TA99) or a platelet integrin antigen (6A6) were grafted onto IgG1, 2a, 2b, or 3 Fc regions and coexpressed with the appropriate light chains (*17*, *18*). These recombinant antibodies were purified, and subsequent testing revealed that switching the constant regions of IgG did not affect antigen binding affinity (*18*) (table S1). As expected, however, specific differences in binding affinity of each subclass to specific FcγRs were observed, resulting in different A/I ratios for each subclass (*17*) (fig. S1, table S2).

To determine whether the differences in A/I ratios for individual subclasses correlate to in vivo biological activity, we investigated the ability of these class-switched antibodies to mediate their specific biological functions: tumor clearance and platelet depletion (*14*, *19*). Both TA99 (Fig. 1, A and B) and 6A6 (Fig. 1C) carrying IgG2a constant regions (A/I = 70) displayed enhanced activity compared with these antibodies bearing IgG1 constant regions (A/I = 0.1). IgG2a and 2b were equivalent in their ability to mediate platelet clearance, whereas IgG2a resulted in enhanced antibody-dependent cellular cytotoxicity (ADCC) in the metastatic melanoma model compared with IgG2b (A/I = 7) (Fig. 1, A and B). The hierarchy of activity for the IgG subclasses in these immune functions was thus IgG2a ≥ IgG2b > IgG1 ≫ IgG3, mirroring the hierarchy based on the A/I ratios (Fig. 1D).

We next tested the mechanism of this observed differential activity by repeating the experiments using strains of mice carrying specific deficiencies in, or blocked activation of, different activating FcγRs or complement components (Fig. 2; fig. S2). No differences in in vivo activity were observed in complement-deficient (C4, C3, or CR1/2) strains (fig. S2). In contrast, IgG1, 2a, and 2b all depended on expression of activating FcγR, because activity was abrogated in the common γ chain–deficient background (Fig. 2, A, B, and E). Because IgG2a has been shown to bind to all of the γ chain–containing activating FcγRs in vitro [with high affinity (10^8 to 10^9 M^{-1}) to FcγRI, intermediate affinity (10^7 M^{-1}) to FcγRIV, and low affinity (10^6 M^{-1}) to FcγRIII], its in vivo capacity to deplete platelets or to mediate ADCC could, in principle, result from engagement of one or more of these FcγRs. We tested the contributions of each of these

Laboratory of Molecular Genetics and Immunology, The Rockefeller University, 1230 York Avenue, New York, NY 10021, USA.

*To whom correspondence should be addressed. E-mail: ravetch@rockefeller.edu

Prostaglandin E_2 Promotes Colon Cancer Cell Growth Through a G_S-Axin-ß-Catenin Signaling Axis

Maria Domenica Castellone, Hidemi Teramoto, Bart O. Williams, Kirk M. Druey and J. Silvio Gutkind

Science **310** (5753), 1504-1510.
DOI: 10.1126/science.1116221originally published online November 17, 2005